Yrast states of even tungsten isotopes $^{170-182}$W

M. R. Gunye and Ashok Kumar
Theoretical Reactor Physics Section, Bhabha Atomic Research Centre, Trombay, Bombay-85, India
(Received 9 July 1979)

The yrast states up to $J = 22^+$ of seven even tungsten isotopes $^{170-182}$W are studied in a microscopic formulation of variation after angular momentum projection with number conservation in each state. The Hamiltonian with quadrupole plus pairing interactions is employed in the calculations of energy spectra, quadrupole moments, and $B(E2)$ values. The results of the calculations are in good agreement with the corresponding experimental data.

[NUCLEAR STRUCTURE W isotopes; calculated energy spectra, quadrupole moments, and $B(E2)$ values. Variation with number-conserved projected states.]

I. INTRODUCTION

The backbending phenomenon observed[1] in some deformed rare-earth nuclei gave a stimulus to study the structure of high-spin states in heavy nuclei. The anomalous backbending behavior at some critical angular momentum $J_c \geq 12$ in the rotational band of many nuclei is interpreted as a manifestation of the Coriolis interaction between the collective and the intrinsic motion of the nucleons. There are two alternative proposals to explain the anomalous behavior in terms of the Coriolis force. Mottelson and Valatin[2] predict the anomalous behavior at some critical high angular momentum as a consequence of the Coriolis antipairing phase transition from the superfluid to the normal nuclear state. The alternative proposal by Stephens and Simon[3] state that certain individual nucleons may respond to the Coriolis force prior to the phase transition proposed by Mottelson and Valatin.[2] This rotation alignment proposal[3] attributes backbending to the Coriolis decoupling of a nucleon pair in orbital with high angular momentum j from the rotating core and subsequent alignment with the core angular momentum. The Coriolis interaction is strong for the substates of high-j orbitals with small projection Ω on the symmetry axis and consequently the decoupled band can drop below the completely paired normal ground band at higher spins, thus causing anomalous behavior.

It is of interest to gain an insight into the intrinsic structure of the high-spin states from the basic microscopic theory. Some attempts[4] have been made to explain the anomalous behavior by using many-body variational methods with constraints. These approaches resort to simplifying approximations[4] regarding angular momentum conservation, leading to errors which could be of the order of magnitude as the observed energy differences to be explained. The recent attempts to understand the structure of high-spin states are based on many-body variational formalism with good angular momentum. This variational method with angular projection has been successfully employed to explain the high-spin yrast states in a few rare-earth nuclei.[5,6] Apart from the complication of angular momentum projection, there is yet another complication due to the number projection[7,8] from the pair-correlated variational state. It is found[8] that the number conservation in each projected angular momentum states improves the quality of the agreement between the theoretical and experimental results.

In this paper, we report the results of the microscopic calculations on the yrast states of seven even-A tungsten isotopes $^{170-182}$W. The nuclei of tungsten, osmium, and platinum form an important region of transition from the deformed rare-earth nuclei to the spherical ^{208}Pb nucelus, and for this reason are of special interest in testing the predictions of different nuclear models. The tungsten isotopes are of vital interest because they bridge the region between the hafnium isotpes exhibiting no backbending, and the osmium and platinum isotpes exhibiting sharp backgending effects. We have therefore studied the even-A tungsten isotopes $^{170-182}$W in order to understand the characteristics of the observed energy spectra of yrast states as a function of the neutron number. The calculations are performed in the framework of a microscopic formalism with variation after angular momentum projection by conserving the nucleon numbers in each projected state. The variational formulation is outlined in Sec. II. The results in the seven tungsten nuclei are discussed in Sec. III and the conclusions are presented in Sec. IV.

II. DESCRIPTION OF CALCULATIONS

A realistic nuclear structure calculation in a microscopic many-body formalism requires a dynamical treatment of a large number of nucleons in a large configuration space. The computational difficulties involved in such a realistic calculation can be reduced by employing a simpler many-body Hamiltonian. In this paper, we use the quadrupole plus pairing interaction Hamiltonian whose parameters are determined by Kumar and Baranger[9] from their study of equilibrium deformations of heavy nuclei:

$$H=\Sigma\epsilon_\alpha a_\alpha^\dagger a_\alpha-\tfrac{1}{2}\chi\Sigma q_{\alpha\gamma}^\mu q_{\delta\beta}^\mu a_\alpha^\dagger a_\beta^\dagger a_\delta a_\gamma -\tfrac{1}{2}G\Sigma(-)^{j_\alpha-m_\alpha+j_\gamma-m_\gamma}a_\alpha^\dagger a_{\bar\alpha}^\dagger a_{\bar\gamma}a_\gamma . \quad (1)$$

Here, q^μ is the quadrupole operator and χ and G are the strengths of quadrupole and pairing interactions respectively. The subscript α in Eq. (1) denotes all the quantum numbers $(n_\alpha, l_\alpha, j_\alpha, m_\alpha)$ necessary for the specification of a spherical single particle state with energy ϵ_α. The state $\bar\alpha$ is connected to the state α by time reversal operator. The intrinsic variational wave function in the present calculations is assumed to be axially symmetric in view of the fact that the nuclei under investigation are found[9] to prefer axially symmetric equilibrium deformations. The trial variational wave function is taken to be the good angular momentum state $\Psi_M^J(\beta,\Delta_p,\Delta_n,\lambda_p,\lambda_n)$ projected from the intrinsic BCS state $\Phi_0(\beta,\Delta_p,\Delta_n,\lambda_p,\lambda_n)$. Thus

$$\Psi_M^J=P_{M0}^J\Phi_0 , \quad (2)$$

where P_{M0}^J is the angular momentum projection operator. The deformation β, the pairing gaps Δ_p and Δ_n, and the chemical potentials λ_p and λ_n are the variational parameters for each angular momentum state J. The suffixes p and n refer to proton and neutron, respectively. The chemical potentials in each state are determined such that the nucleon numbers in each projected state are equal to the actual nucleon numbers in the nucleus. The expectation value E^J of the Hamiltonian in Eq. (1) with respect to the wave function in Eq. (2) can be expressed[6] as

$$E^J(\beta,\Delta_p,\Delta_n,\lambda_p,\lambda_n)=h^J/p^J , \quad (3)$$

where

$$h^J=(J+\tfrac{1}{2})\int_0^\pi d_{00}^J(\theta)(\det W)^{1/2}X(\theta)\sin\theta\,d\theta , \quad (4)$$

$$X(\theta)=2\Sigma\epsilon_i\rho_{i+i+}-G(\Sigma\sigma_{i+i-})^2 -\tfrac{1}{2}\chi(Q_{0+}{}^2+2Q_{2+}{}^2+2Q_{1-}{}^2) , \quad (5)$$

and p^J is obtained from Eq. (4) by replacing $X(\theta)$ by unity. The overlap matrix W in Eq. (4) and the generalized density matrices ρ and σ in Eq. (5) depend[6] on the transformation coefficients of deformed single particle orbits in terms of the spherical basis states, the rotation matrix $d(\theta)$, and the occupation probabilities of the single particle orbits in the intrinsic state Φ_0. The quantities $Q_{\mu\pm}$ in Eq. (5) are given by

$$Q_{\mu\pm}=\Sigma(q_{i\pm j+}^\mu+q_{j+i\pm}^\mu)\rho_{j+i\pm} . \quad (6)$$

The subscript (+ and −) in Eqs. (5) and (6) indicates the states from two subsets that are connected by time reversal operator.

The number of protons Z^J in the projected state with angular momentum J is obtained by evaluating the integral

$$Z^J(\beta,\Delta_p,\Delta_n,\lambda_p,\lambda_n) =(J+\tfrac{1}{2})(p^J)^{-1}\int_0^\pi d_{00}^J(\theta)(\det W)^{1/2} \times\Sigma\rho_{i+i+}\sin\theta\,d\theta . \quad (7)$$

The summation in Eq. (7) over proton (neutron) states gives the proton (neutron) number $Z^J(N^J)$ in the state J. Finally, the $B(E2)$ value for the γ-transition from the initial state J_i to the final state J_f is given by

$$B(E2;J_i\to J_f)=\frac{2J_f+1}{2J_i+1}(p^{J_i}p^{J_f})^{-1}[Q(J_i\to J_f)]^2 , \quad (8)$$

where

$$Q(J_i\to J_f)=\sum_{\mu=0}^{2}(2-\delta_{\mu0})(J_i\mu,2-\mu\,|J_f0) \times(J_i+\tfrac{1}{2})\int_0^\pi d_{-\mu0}^{J_i}(\theta)(\det W)^{1/2} \times(Q_{\mu+}+Q_{\mu-})\sin\theta\,d\theta . \quad (9)$$

Here $(J_i\mu,2-\mu\,|J_f0)$ is the Clebsch-Gordan coefficient and $Q_{\mu\pm}$ is given by Eq. (6).

III. RESULTS AND DISCUSSION

The calculations in the even-A tungsten nuclei $^{170\text{-}182}$W reported in this paper are performed by employing the nuclear Hamiltonian in Eq. (1) with strength parameters χ and G determined by Kumar and Baranger.[9] The same configuration space and the same inert core as specified by them has been considered in the present calculations. The nuclear energies are calculated by minimizing E^J in Eq. (3) by varying the deformation β, the pairing gaps Δ_p and Δ_n, and the chemical potentials λ_p and λ_n for each angular momentum state J. For each set of the values of β, Δ_p, and Δ_n, the chemical potentials λ_p and λ_n are varied so as to yield the

TABLE I. The deformation β, the pairing gaps Δ_p and Δ_n, the energy E_{norm} obtained from the renormalization procedure, the experimental energy E_{expt}, the quadrupole moment $Q(J)$, and the $B(E2;\ J \rightarrow J-2)$ value for each angular momentum state J in ^{170}W.

J	β	Δ_p (MeV)	Δ_n (MeV)	E_{norm} (MeV)	E_{expt} (MeV)	$-Q(J)$ (e b)	$B(E2;\ J \rightarrow J-2)$ (e^2b^2)
0	0.24	1.00	0.92	0.00	0.00		
2	0.24	1.00	0.92	0.13	0.16	1.59	0.62
4	0.27	0.99	0.83	0.41	0.46	2.02	0.89
6	0.27	0.99	0.83	0.83	0.87	2.22	0.99
8	0.27	0.99	0.58	1.32	1.36	2.34	1.04
10	0.27	0.99	0.33	1.86	1.90	2.43	1.08
12	0.27	0.99	0.00	2.38	2.46	2.46	1.08
14	0.24	1.00	0.00	2.87	2.90	2.33	0.96
16	0.24	1.00	0.00	3.39	3.34	2.36	0.97
18	0.24	1.00	0.00	3.97	3.87	2.37	0.98
20	0.24	0.69	0.00	4.59	4.49	2.38	0.99
22	0.24	0.69	0.00	5.24	5.18	2.38	1.00

correct number Z of protons and N of neutrons for each state J. The numbers Z^J and N^J computed from Eq. (7) are very sensitively dependent on λ_p and λ_n. Consequently, it is necessary to incorporate very find variations of λ_p and λ_n in the variational procedure so as to obtain the correct number in each projected angular momentum state. In the present calculations, we have achieved an accuracy up to the fourth decimal place in the nucleon numbers computed in each J state.

The values of the strength parameters χ and G are estimated by Kumar and Baranger[9] in a truncated configuration space of two major shells each for protons and neutrons by assuming an inert core with $Z=40$ and $N=70$. The assumption of the inert core necessitates the modification of the nucleon charges and the excitation energies. As is the standard practice,[9] we replace bare nucleon charges by effective charges to simulate the effects of core-polarization and configuration truncation. The simplest way to incorporate the effect of the neglected core on the projected energies is by renormalizing the calculated energy spectrum. We achieve it by introducing a parameter, namely the moment of inertia I_{core}. The moment of inertia of the nucleus is assumed to be the sum of the moment of inertia I_{core} of the core and I_{calc} of the outer nucleons. The energy E^J_{calc}, computed by considering only the outer valence nucleons can be expressed as

$$E^J_{\text{calc}} = \frac{\hbar^2}{2I_{\text{calc}}} J(J+1)\,,$$

and similarly, the corrected or the renormalized energy can be expressed as

$$E^J_{\text{norm}} = \frac{\hbar^2}{2(I_{\text{core}}+I_{\text{calc}})} J(J+1)\,.$$

TABLE II. The deformation β, the pairing gaps Δ_p and Δ_n, the energy E_{norm} obtained from the renormalization procedure, the experimental energy E_{expt}, the quadrupole moment $Q(J)$, and the $B(E2;\ J \rightarrow J-2)$ value for each angular momentum state J in ^{172}W.

J	β	Δ_p (MeV)	Δ_n (MeV)	E_{norm} (MeV)	E_{expt} (MeV)	$-Q(J)$ (e b)	$B(E2;\ J \rightarrow J-2)$ (e^2b^2)
0	0.28	0.97	0.77	0.00	0.00		
2	0.28	0.97	0.77	0.11	0.12	1.67	0.68
4	0.28	0.97	0.77	0.37	0.38	2.12	0.98
6	0.28	0.97	0.77	0.75	0.73	2.33	1.08
8	0.28	0.97	0.54	1.21	1.15	2.47	1.15
10	0.28	0.97	0.31	1.68	1.62	2.56	1.19
12	0.28	0.97	0.00	2.16	2.13	2.62	1.22
14	0.28	0.97	0.00	2.67	2.68	2.65	1.24
16	0.28	0.97	0.00	3.26	3.26	2.68	1.25
18	0.28	0.97	0.00	3.90	3.85	2.70	1.27
20	0.28	0.68	0.00	4.60	4.50	2.69	1.25
22	0.28	0.68	0.00	5.36		2.70	1.25

TABLE III. The deformation β, the pairing gaps Δ_p and Δ_n, the energy E_{norm} obtained from the renormalization procedure, the experimental energy E_{expt}, the quadrupole moment $Q(J)$, and the $B(E2;\ J \rightarrow J-2)$ value for each angular momentum state J in ^{174}W.

J	β	Δ_p (MeV)	Δ_n (MeV)	E_{norm} (MeV)	E_{expt} (MeV)	$-Q(J)$ (e b)	$B(E2;\ J \rightarrow J-2)$ (e^2b^2)
0	0.29	0.95	0.72	0.00	0.00		
2	0.29	0.95	0.72	0.11	0.11	1.74	0.75
4	0.29	0.95	0.72	0.35	0.36	2.21	1.07
6	0.29	0.95	0.72	0.72	0.71	2.44	1.19
8	0.29	0.95	0.50	1.18	1.14	2.58	1.25
10	0.29	0.95	0.29	1.67	1.64	2.68	1.30
12	0.29	0.95	0.00	2.18	2.19	2.74	1.32
14	0.29	0.95	0.00	2.68	2.79	2.79	1.34
16	0.29	0.95	0.00	3.28	3.40	2.82	1.36
18	0.29	0.95	0.00	3.92	3.98	2.84	1.37
20	0.29	0.95	0.00	4.64	4.61	2.86	1.39
22	0.29	0.95	0.00	5.41	5.32	2.88	1.41

Since the calculated energy E^J_{calc} deviates from the pure rotational pattern, the moment of inertia I_{calc} varies with the angular momentum J. The moment of inertia I_{core}, however, may not vary with J and can be assumed to be constant, at least for a set of states. The present calculations in the seven tungsten nuclei indicate that I_{core} is nearly constant for all values of J. The calculated energy spectrum in each nucleus is renormalized by choosing the parameter I_{core} so as to obtain an overall agreement with the experimental energy spectrum, rather than reproducing the excitation energy of a particular state. It is gratifying to note that the experimental energy spectra of the yrast states up to $J \leq 22^+$ in all the tungsten nuclei under investigation are reproduced by employing nearly a constant value $I_{\text{core}} = (10 \pm 1)\hbar^2/\text{MeV}$ in the renormalization calculation.

The renormalized energy and the variational parameters β, Δ_p, and Δ_n corresponding to the minimum of energy for each angular momentum state J are shown in Tables I to VII for all the even-A tungsten nuclei from ^{170}W to ^{182}W, respectively. It can be seen from these tabulations that the renormalized energies are in good agreement with the corresponding experimental energies,[10] the maximum deviation being about 100 keV in any one of the seven tungsten isotopes under consideration here. In order to visualize the agreement between the calculated and experimental energy spectra at a glance, we have plotted the energy $E(J)$ as a function of $J(J+1)$ in Fig. 1 for ^{170}W, Fig. 2 for ^{172,174}W, Fig. 3 for ^{176,178}W, and Fig. 4 for ^{180,182}W. These figures bring out the salient feature of a departure of the energy spectra from the simple rotational structure based on a single band. The anomalous backbending is observed experimentally in ^{170}W at the critical angular momen-

TABLE IV. The deformation β, the pairing gaps Δ_p and Δ_n, the energy E_{norm} obtained from the renormalization procedure, the experimental energy E_{expt}, the quadrupole moment $Q(J)$, and the $B(E2;\ J \rightarrow J-2)$ value for each angular momentum state J in ^{176}W.

J	β	Δ_p (MeV)	Δ_n (MeV)	E_{norm} (MeV)	E_{expt} (MeV)	$-Q(J)$ (e b)	$B(E2;\ J \rightarrow J-2)$ (e^2b^2)
0	0.29	0.93	0.70	0.00	0.00		
2	0.29	0.93	0.70	0.11	0.11	1.76	0.76
4	0.29	0.93	0.70	0.35	0.35	2.24	1.09
6	0.29	0.93	0.70	0.72	0.70	2.47	1.21
8	0.29	0.93	0.49	1.18	1.14	2.61	1.28
10	0.29	0.93	0.28	1.67	1.65	2.72	1.34
12	0.29	0.93	0.00	2.17	2.21	2.79	1.37
14	0.29	0.93	0.00	2.73	2.80	2.83	1.40
16	0.29	0.93	0.00	3.37	3.43	2.86	1.41
18	0.29	0.93	0.00	4.08	4.00	2.89	1.42
20	0.29	0.93	0.00	4.85		2.91	1.44
22	0.29	0.64	0.00	5.74		2.92	1.45

TABLE V. The deformation β, the pairing gaps Δ_p and Δ_n, the energy E_{norm} obtained from the renormalization procedure, the experimental energy E_{expt}, the quadrupole moment $Q(J)$, and the $B(E2;\ J \rightarrow J-2)$ value for each angular momentum state J in ^{178}W.

J	β	Δ_p (MeV)	Δ_n (MeV)	E_{norm} (MeV)	E_{expt} (MeV)	$-Q(J)$ (e b)	$B(E2;\ J \rightarrow J-2)$ (e^2b^2)
0	0.27	0.89	0.78	0.00	0.00		
2	0.27	0.89	0.78	0.11	0.11	1.69	0.70
4	0.27	0.89	0.78	0.35	0.34	2.14	1.00
6	0.30	0.91	0.71	0.73	0.70	2.54	1.28
8	0.30	0.91	0.50	1.18	1.14	2.68	1.35
10	0.30	0.91	0.29	1.70	1.67	2.77	1.39
12	0.27	0.89	0.00	2.25	2.25	2.63	1.24
14	0.27	0.89	0.00	2.81	2.86	2.67	1.25
16	0.27	0.89	0.00	3.44	3.49	2.70	1.27
18	0.27	0.63	0.00	4.13		2.71	1.26
20	0.27	0.63	0.00	4.88		2.72	1.27
22	0.27	0.63	0.00	5.70		2.73	1.28

tum $J_c = 12$ and in ^{174,176}W at $J_c = 16$. The backbending behavior is conventionally illustrated by the familiar S-shaped plot of the moment of inertia I as a function of the square of the rotational frequency ω. It should be stressed here that the calculated energies should be in very good agreement with the experimental energies so as to reproduce the characteristic experimental backbending curve. Since the microscopic calculations with the simple quadrupole plus pairing force model cannot yield such precise agreement, one can expect to see only the trend of the I vs ω^2 curve. The theoretical and experimental backbending curves in ^{170}W and ^{174}W are displayed in Figs. 5 and 6 respectively, for comparison.

It is seen from the results shown in Tables II, III, IV, and VII that the deformation parameter remains constant for all the yrast states in ^{172}W, ^{174}W, ^{176}W, and ^{182}W with the value 0.28, 0.29, 0.29, and 0.26, respectively. In the case of ^{180}W shown in Table VI, the deformation is constant ($\beta = 0.27$) for all the states with $J \leq 14$ and then suddenly decreases to $\beta = 0.24$, remaining constant for all the higher spin states. In ^{170}W and ^{178}W, the deformation is constant for all the angular momentum states except those with $4 \leq J \leq 12$ for which it assumes a larger value, as seen from Tables I and V, respectively.

The pairing gap Δ_p for protons remains nearly constant for almost all the yrast states in the tungsten nuclei under investigation. A slight reduction in the value of Δ_p is observed in ^{170,172,178,180}W only for high-spin states with $J \geq 18$. The situation is, however, different for the pairing gap Δ_n for neutrons. The pattern of the variation of Δ_n with J is same for all the seven tungsten iso-

TABLE VI. The deformation β, the pairing gaps Δ_p and Δ_n, the energy E_{norm} obtained from the renormalization procedure, the experimental energy E_{expt}, the quadrupole moment $Q(J)$, and the $B(E2;\ J \rightarrow J-2)$ value for each angular momentum state J in ^{180}W.

J	β	Δ_p (MeV)	Δ_n (MeV)	E_{norm} (MeV)	E_{expt} (MeV)	$-Q(J)$ (e b)	$B(E2;\ J \rightarrow J-2)$ (e^2b^2)
0	0.27	0.87	0.78	0.00	0.00		
2	0.27	0.87	0.78	0.11	0.10	1.68	0.69
4	0.27	0.87	0.78	0.35	0.34	2.14	1.00
6	0.27	0.87	0.78	0.73	0.69	2.35	1.10
8	0.27	0.87	0.54	1.18	1.14	2.48	1.16
10	0.27	0.87	0.31	1.70	1.66	2.55	1.20
12	0.27	0.87	0.00	2.24	2.24	2.60	1.21
14	0.27	0.87	0.00	2.81	2.83	2.64	1.23
16	0.24	0.62	0.00	3.44	3.42	2.52	1.25
18	0.24	0.62	0.00	4.13	4.02	2.53	1.13
20	0.24	0.62	0.00	4.88		2.54	1.14
22	0.24	0.62	0.00	5.69		2.54	1.14

TABLE VII. The deformation β, the pairing gaps Δ_p and Δ_n, the energy E_{norm} obtained from the renormalization procedure, the experimental energy E_{expt}, the quadrupole moment $Q(J)$, and the $B(E2;\ J \rightarrow J-2)$ value for each angular momentum state J in ^{182}W. The numbers in bracket indicate the experimental $B(E2)$ values.

J	β	Δ_p (MeV)	Δ_n (MeV)	E_{norm} (MeV)	E_{expt} (MeV)	$-Q(J)$ (e b)	$B(E2;\ J \rightarrow J-2)$ (e^2b^2)
0	0.26	0.85	0.81	0.00	0.00		
2	0.26	0.85	0.81	0.11	0.10	1.64	0.66
							(0.84 ± 0.02) [a]
4	0.26	0.85	0.81	0.37	0.33	2.09	0.95
							(1.15 ± 0.08) [a]
6	0.26	0.85	0.81	0.77	0.68	2.29	1.05
							(1.16 ± 0.12) [a]
8	0.26	0.85	0.57	1.25	1.14	2.41	1.11
							(1.47 ± 0.10) [b]
10	0.26	0.85	0.33	1.79	1.71	2.49	1.15
							(1.49 ± 0.12) [b]
12	0.26	0.85	0.00	2.34	2.37	2.45	1.17
							(1.11 ± 0.28) [b]
14	0.26	0.85	0.00	2.98	3.11	2.58	1.19
16	0.26	0.85	0.00	3.69		2.60	1.21
18	0.26	0.85	0.00	4.49		2.61	1.22
20	0.26	0.85	0.00	5.37		2.50	1.10

[a] Reference 11.
[b] Reference 12.

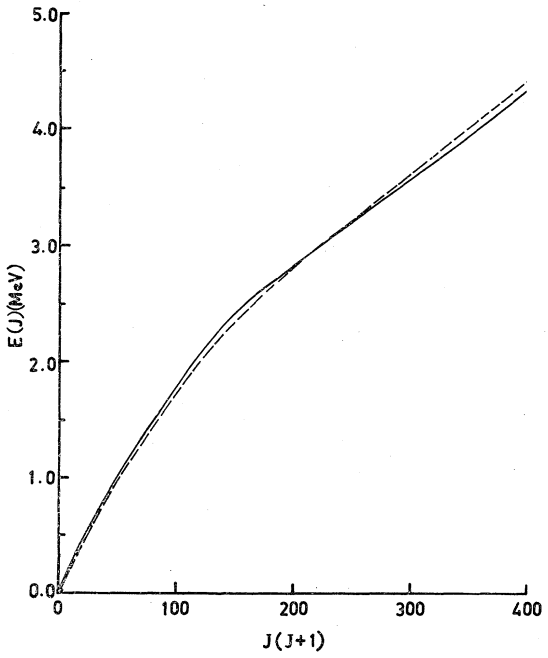

FIG. 1. The calculated (dotted curve) and the experimental (solid curve) values of the energy $E(J)$ for each angular momentum state J in ^{170}W are plotted as a function of $J(J+1)$.

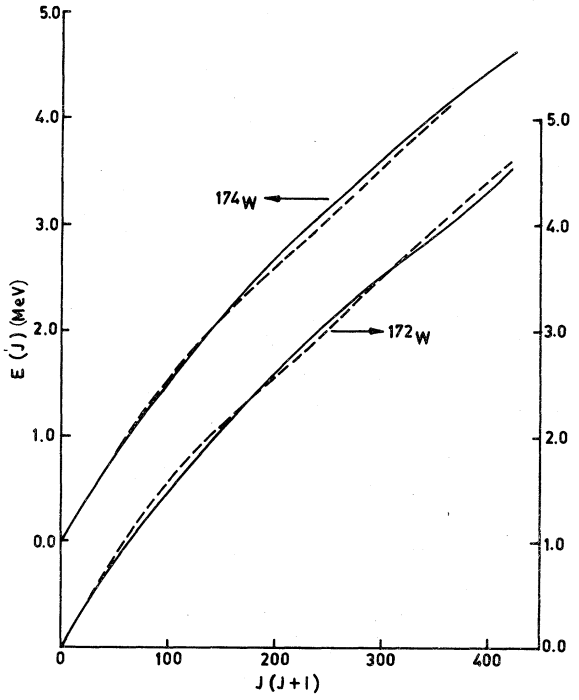

FIG. 2. The calculated (dotted curve) and the experimental (solid curve) values of the energy $E(J)$ for each angular momentum state J in ^{172}W (right) and ^{174}W (left) are plotted as a function of $J(J+1)$.

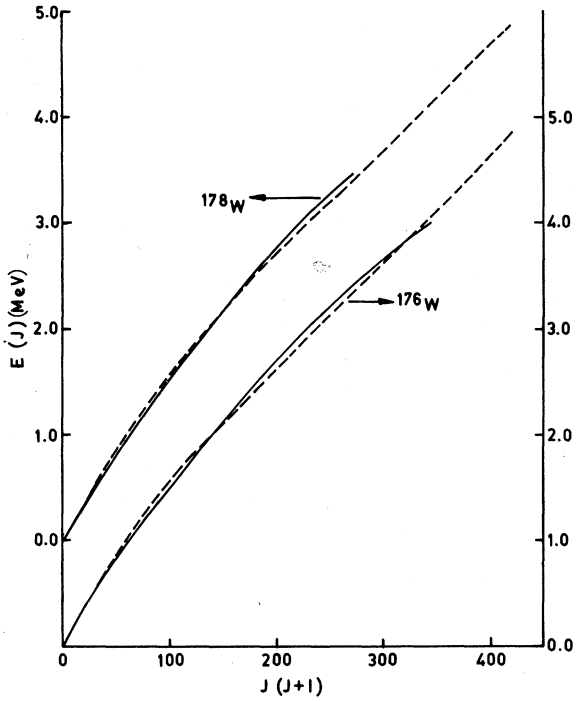

FIG. 3. The calculated (dotted curve) and the experimental (solid curve) values of the energy $E(J)$ for each angular momentum state J in ^{176}W (right) and ^{178}W (left) are plotted as a function of $J(J+1)$.

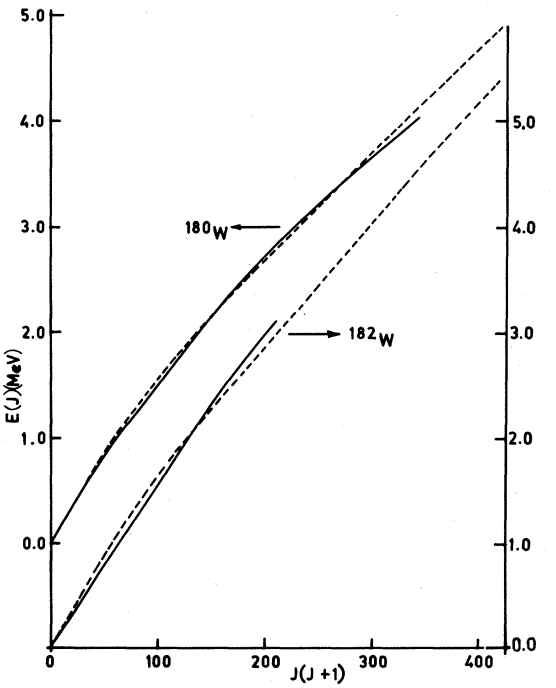

FIG. 4. The calculated (dotted curve) and the experimental (solid curve) values of the energy $E(J)$ for each angular momentum state J in ^{180}W (left) and ^{182}W (right) are plotted as a function of $J(J+1)$.

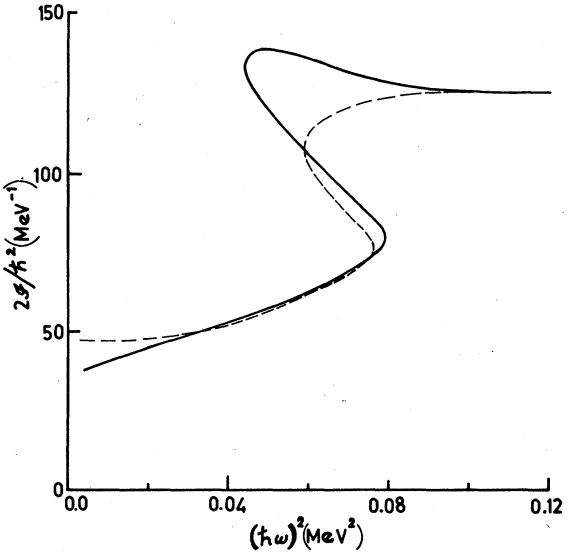

FIG. 5. The calculated (dotted) and the experimental (solid) curves of the moment of inertia as a function of the square of rotational frequency are plotted in the case of ^{170}W.

topes. In each case, the pairing gap Δ_n remains constant for the first few yrast states and then decreases with the increase in J value until it vanishes suddenly at the critical value $J_C = 12$ so as to remain zero for all higher spin states. Although the pairing gap Δ_n vanishes at $J_C = 12$ for all the tungsten isotopes under consideration here, the backbending is established only in ^{170,174,176}W.

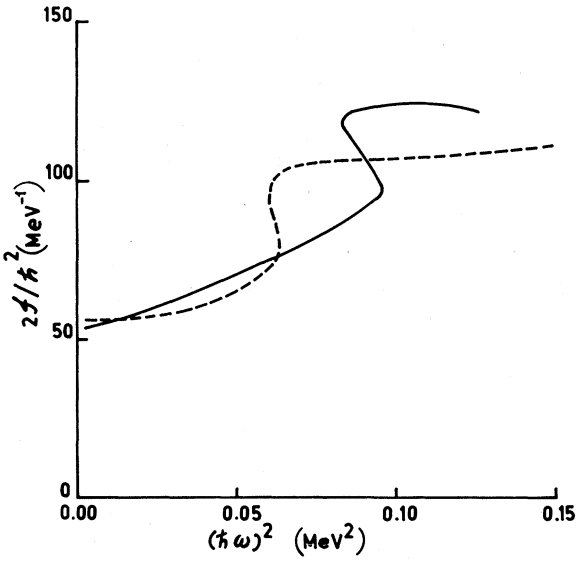

FIG. 6. The calculated (dotted) and the experimental (solid) curves of the moment of inertia as a function of the square of rotational frequency are plotted in the case of ^{174}W.

It is thus clear that the vanishing of the neutron pairing gap at some critical value of the angular momentum does not necessarily indicate the backbending behavior.

The backbending in a particular nucleus would depend in detail on the structure of single particle orbitals near the Fermi surface of nucleons. It is thus worthwhile to discuss the single particle states in the vicinity of the Fermi surface of nucleons. This may give some insight into the phenomenological approach[3] based on decoupling of bands where the Coriolis effects in high-j single particle orbitals are assumed to play an important role. It may be mentioned, however, that the following discussion is only qualitative. The present microscopic approach uses the same variational parameter Δ_p for all proton levels and the same parameter Δ_n for all neutron levels. It is therefore not possible to conclude decisively about the role of the decoupling of the pair of nucleons from individual single particle orbitals in backbending phenomenon. The proton and neutron orbitals near the Fermi surface of tungsten nuclei under investigation are displayed in Figs. 7 and 8, respectively. It is seen from Fig. 7 that, in the range of deformation β relevant for these nuclei, the only high-j orbital near the Fermi surface of protons is the $\Omega = \frac{9}{2}$ substate predominantly (99.6%) from the $h_{11/2}$ state. Since the Coriolis force is weak for high $-\Omega$ substates, the backbending cannot probably result from a decoupling of a proton pair

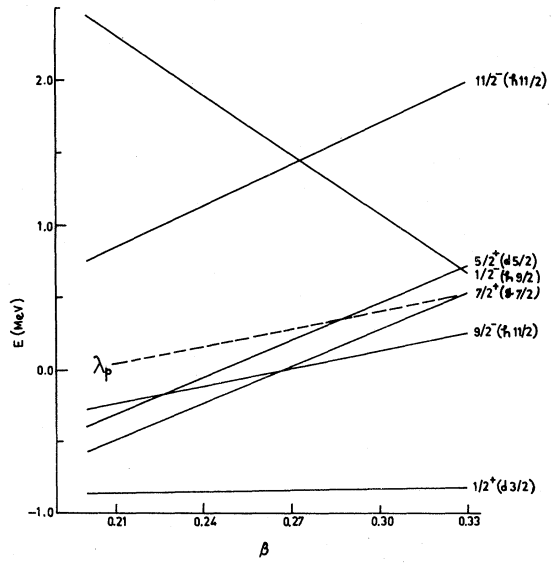

FIG. 7. The energies (in MeV) of the deformed orbitals near the Fermi level λ_p for protons (dotted curve) in tungsten nuclei are shown as a function of deformation β. The Ω^π values and the predominant basis state with the largest amplitude in the wave function of the orbital are shown on the right.

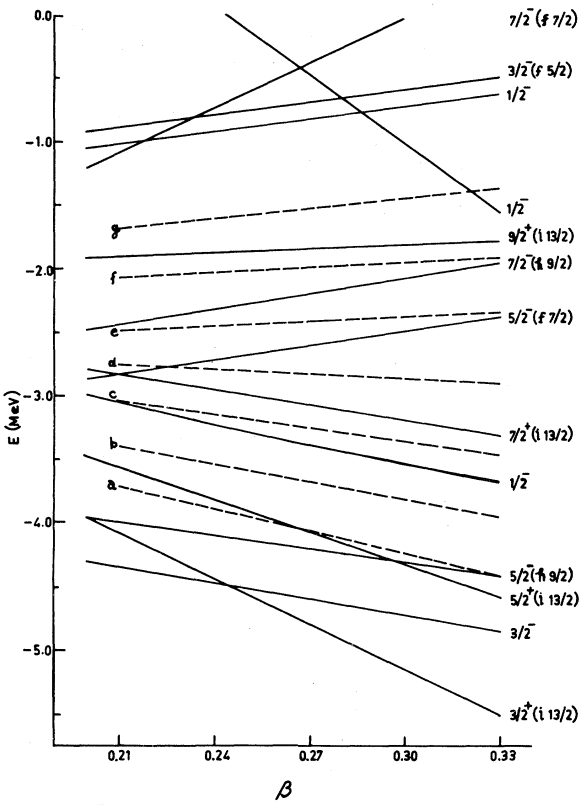

FIG. 8. The energies (in MeV) of the deformed orbitals near the Fermi level for neutrons in tungsten nuclei are shown as a function of deformation β. The Ω^π value and the predominant basis state with the largest amplitude in the wave function of the orbital are shown on the right. The dotted curves a, b, c, d, e, f, and g indicate the Fermi levels in the even tungsten isotopes from ^{170}W to ^{182}W, respectively.

from this $h_{11/2}$ orbital near the proton Fermi surface. Regarding the neutron states (Fig. 8) near the Fermi surface, the situation is rather different. In the case of ^{170}W, the high-j orbitals near the neutron Fermi surface are the $\Omega = \frac{5}{2}^+$ substate predominantly (93.5%) from $i_{13/2}$ state and $\Omega = \frac{5}{2}^-$ substate predominantly (77.4%) from $h_{9/2}$ state. The substates $\Omega = \frac{7}{2}^+$ and $\Omega = \frac{9}{2}^+$ predominantly (96.4% and 98.1%) from $i_{13/2}$ state are in the vicinity of the neutron Fermi surface of ^{174,176}W and ^{180,182}W, respectively. Since the Coriolis force is strong if the Fermi surface is close to the low-Ω substates ($\Omega \leq \frac{5}{2}$) of the high-j state, one can expect the occurrence of backbending in ^{170}W. It should, however, be noted that the $\Omega = \frac{5}{2}$ substate is not far away from the neutron Fermi surface of ^{172}W which does not exhibit backbending. The observed backbending in ^{174,176}W at comparatively high angular momentum $J_c = 16$ can be due to the presence of $\Omega = \frac{7}{2}$ substate of $i_{13/2}$ orbit near the

Fermi surface. The presence of the $\Omega = \frac{9}{2}$ substate near the Fermi surface of ^{180,182}W does not result in backbending since the Coriolis force is weak for high $-\Omega$ substates of high-j orbits.

The quadrupole moment $Q(J)$ and the $B(E2; J \rightarrow J-2)$ values are calculated by employing the number-conserved projected wavefunctions for each angular momentum state. The effects of core polarization are simulated by ascribing effective charges[9] $e_p = (1 + 1.5Z/A)e$ for protons and $e_n = (1.5Z/A)e$ for neutrons. The computed values of $Q(J)$ and $B(E2)$ in the tungsten nuclei are shown in Tables I to VII. The experimental data in these nuclei with the exception of ^{182}W are, however, not available. The calculated $B(E2)$ values agree well with the corresponding experimental values available in ^{182}W.

In order to understand the connection between the Bohr-Mottelson collective model and the microscopic approach followed in this paper, we have calculated the intrinsic quadrupole moment Q_0 from $Q(J)$ values as well as from $B(E2)$ values, using the following relations from the collective model:

$$Q(J) = -\frac{J}{2J+3} Q_0 ,$$

$$B(E2; J \rightarrow J-2) = \frac{15}{32\pi} \frac{J(J-1)}{(2J-1)(2J+1)} Q_0^2 .$$

It is found that in all the seven tungsten nuclei under consideration, the $Q_0(Q)$ value extracted from the quadrupole moment $Q(J)$ agrees very well with the corresponding value $Q_0(E2)$ obtained from $B(E2)$ value. In general, $Q_0(Q)$ is very slightly less than the corresponding $Q_0(E2)$ value, the maximum difference being about 0.1 e b. The present calculations indicate a systematic trend in the behavior of both Q_0 values as deformation changes for different angular momentum states. We find that the value of the intrinsic quadrupole moment Q_0 increases from ^{170}W to ^{176}W and then decreases from ^{176}W to ^{182}W. The average values of Q_0 obtained from the present calculations are 5.6 e b in ^{170}W, 6.2 e b in ^{176}W, and 5.7 e b in ^{182}W.

IV. CONCLUSION

The microscopic formalism of variation with number-conserved projected states is applied to study the yrast states of seven even-A tungsten nuclei $^{170-182}$W. The energy spectra, quadrupole moments, and $B(E2)$ values are calculated by employing the Hamiltonian with quadrupole plus pairing interactions. The deformation β, pairing gaps Δ_p and Δ_n, and the chemical potentials λ_p and λ_n are varied to obtain the energy minimum and to conserve the number of nucleons in each angular momentum state. The effect of core polarization is simulated by ascribing effective charges to the nucleons and by introducing the moment of inertia of the core to renormalize the energy spectra. The experimental energy spectra of the yrast states in all the tungsten nuclei under investigation are reproduced well by using nearly a constant value for the moment of inertia of the core. The present calculations indicate that the vanishing of the neutron pairing gap Δ_n at some critical angular momentum J_C is not a sufficient condition for backbending behavior in nuclei. The single particle orbitals in the vicinity of the neutron Fermi surface play an important role in the backbending behavior observed in ^{170,174,176}W.

[1] R. A. Sorensen, Rev. Mod. Phys. 45, 353 (1973); A. Johnson and Z. Szymanski, Phys. Rep. 7C, 181 (1973).
[2] B. R. Mottelson and J. G. Valatin, Phys. Rev. Lett. 5, 511 (1960).
[3] F. S. Stephens and R. S. Simon, Nucl. Phys. A183, 257 (1972).
[4] K. Kumar, Phys. Scr. 6, 270 (1972); S. C. K. Nair and A. Ansari, Phys. Lett. 47B, 200 (1973); B. Banerjee, M. Mang, and P. Ring, Nucl. Phys. A215, 366 (1973).
[5] A. Faessler, F. Grummer, L. Lin, and J. Urbano, Phys. Lett. 48B, 87 (1974).
[6] C. S. Warke and M. R. Gunye, Phys. Rev. C 12, 1647 (1975); 13, 859 (1976).
[7] F. Grummer, K. W. Schimid, and A. Faessler, Nucl. Phys. A239, 289 (1975).
[8] M. R. Gunye and C. S. Warke, J. Phys. G 5, L83 (1979).
[9] K. Kumar and M. Baranger, Nucl. Phys. A110, 529 (1968).
[10] R. O. Sayer, J. S. Smith, and W. T. Milner, At. Data Nucl. Data Tables 15, 85 (1975); F. M. Bernthal, C. L. Dors, B. Jeltena, T. L. Khoo, and R. A. Warner, Phys. Lett. 64B, 147 (1976); G. D. Dracoulis, P. M. Walker, and A. Johnston, J. Phys. G 4, 713 (1978).
[11] W. T. Milner, F. K. McGowan, R. L. Robinson, P. H. Stelson, and R. O. Sayer, Nucl. Phys. A177, 1 (1971).
[12] Ph. Hubert, C. Roulet, H. Sergolle, P. Colombani, J. M. Lagrange, V. Vanhorenbeeck, and N. R. Johnson, Nucl. Phys. A321, 213 (1979).